JGR Earth Surface

RESEARCH ARTICLE
10.1029/2021JF006066

Barrier Breaching Versus Overwash Deposition: Predicting the Morphologic Impact of Storms on Coastal Barriers

Jaap H. Nienhuis[1], **Leoni G. H. Heijkers**[1], **and Gerben Ruessink**[1]

[1]Department of Physical Geography, Utrecht University, Utrecht, the Netherlands

Key Points:

- New analytical theory compares overwashing flow against barrier volume to predict breaching and washover deposition
- We test our theory against Delft3D simulations and Hurricane Sandy observations: vegetation and island elevation help to prevent breaching
- Developed barrier islands do not follow predicted trends, suggesting alternative controls on overwashing and breaching

Supporting Information:

Supporting Information may be found in the online version of this article.

Correspondence to:

J. H. Nienhuis,
j.h.nienhuis@uu.nl

Citation:

Nienhuis, J. H., Heijkers, L. G. H., & Ruessink, G. (2021). Barrier breaching versus overwash deposition: Predicting the morphologic impact of storms on coastal barriers. *Journal of Geophysical Research: Earth Surface*, *126*, e2021JF006066. https://doi.org/10.1029/2021JF006066

Received 11 JAN 2021
Accepted 19 MAY 2021

Abstract Waves and water level setup during storms can create overwashing flows across barrier islands. Overwashing flows can cause erosion, barrier breaching, and inlet formation, but their sediments can also be deposited and form washover fans. These widely different outcomes remain difficult to predict. Here we suggest that a breach develops when the sediment volume transported by overwashing flows exceeds the barrier subaerial volume. We form a simple analytical theory that estimates overwashing flows from storm characteristics, barrier morphology, and dune vegetation, and which can be used to assess washover deposition and breaching likelihood. Our theory suggests that barrier width and storm surge height are two important controls on barrier breaching. We test our theory with the hydrodynamic and morphodynamic model Delft3D as well as with field observations of 21 washover fans and 6 breaches that formed during Hurricane Sandy. There is reasonable correspondence for natural but not for developed barrier coasts, where traditional sediment transport equations do not readily apply. Our analytical formulations for breach formation and overwash deposition can be used to improve long-term barrier island models.

Plain Language Summary Storms can have big impacts on coastlines. Beaches and dunes can be eroded, their sands can be blown inland, coverings houses and streets. Sometimes, there is so much erosion that new channels have formed that breach the island and make a new connection between the ocean and the lagoon. Here, we develop and test a new theory to predict these outcomes ahead of time. We find that high storm surges along narrow dunes are most vulnerable to breaching.

1. Introduction

Storms can have large impacts on barrier islands. Overwashing flows and waves can move sediment across barrier islands and result in washover deposition (Figure 1a) or barrier island breaching (Figure 1b) (Pierce, 1970). These outcomes are strongly sensitive to barrier characteristics and storm intensity (Suter et al., 1982; Plomaritis et al., 2018). Hurricane (also called "superstorm") Sandy hit the US East Coast in 2012 and resulted in widespread overwashing and numerous breaches (Figure 1) (Sopkin et al., 2014). Breaching is likely to become more common as a result of sea-level rise and barrier island flooding (Nienhuis & Lorenzo-Trueba, 2019a; Passeri et al., 2020). At the same time, washover deposition is a critical landward-directed sediment flux that can support barrier aggradation and prevent barrier drowning. Reliable predictions of barrier breaching and washover deposition, whether for long-term models or short-term assessment before landfall, remain difficult.

In this study, we propose that storms make barrier islands breach when the cumulative sediment flux of an overwashing flow exceeds the barrier subaerial volume. Conversely, a washover deposit will form when an overwashing flow does not erode the barrier down to sea level, with increasing washover volumes as overwashing flows approach the washover-to-breaching threshold.

The objective of this study is to test this theory using Delft3D simulations complemented with observations from Hurricane Sandy. We systematically explore the effect of barrier island morphology, storm characteristics, and dune vegetation on overwashing flows and the morphologic response of barrier coasts.

Figure 1. Storm response to Hurricane Sandy, showing (a) the deposition of a washover fan and (b) the formation of a breach. Inset shows their location in the North East USA. These examples are #24 and #1, respectively, of the Supporting Data Table. Pre-storm images from Google Earth, post-storm images from NOAA Emergency Response Imagery (https://storms.ngs.noaa.gov/).

2. Background

2.1. Overwashing Flows

Overwashing flows occur when wave runup and/or water levels exceed the island elevation and produce a water surface slope across the island (Fisher & Stauble, 1977; Kobayashi, 2010). High water levels often result from storm winds that generate surges and waves, and their impact is often assessed based on relative elevation of wave runup and water levels against the dune crest (Sallenger, 2000).

Overwashing flows and sediment transport have been studied in the laboratory and in the field (see Donnelly et al., 2006 for a review). They are highly variable over time and space and can flow in both directions across barrier islands (Goff et al., 2019; Wesselman et al., 2018) depending on storm characteristics and the (storm and tide-induced) phase lag of lagoon water levels compared to the ocean (Shin, 1996).

Several studies have aimed to determine the relative influence of wind, waves, infragravity waves, and water level gradients on water and sediment fluxes transported in overwashing flows. A recent study by Engelstad et al. (2018) on an overwashing flow across the Dutch island of Schiermonnikoog showed that sediment transport was primarily controlled by currents, but that occasional high sediment concentrations were found on wave infragravity timescales. Wave conditions (McCall et al., 2010) and foredune size (de Winter et al., 2015) are important controls on foredune erosion and determining locations of overwashing flows, whereas the water level gradient controlled the amount of overwashing sediment and its deposition in the back barrier (Engelstad et al., 2018; McCall et al., 2010). The evolution and magnitude of overwashing flows also depend on dune morphology and vegetation patterns (Houser et al., 2008; Kobayashi, 2010;

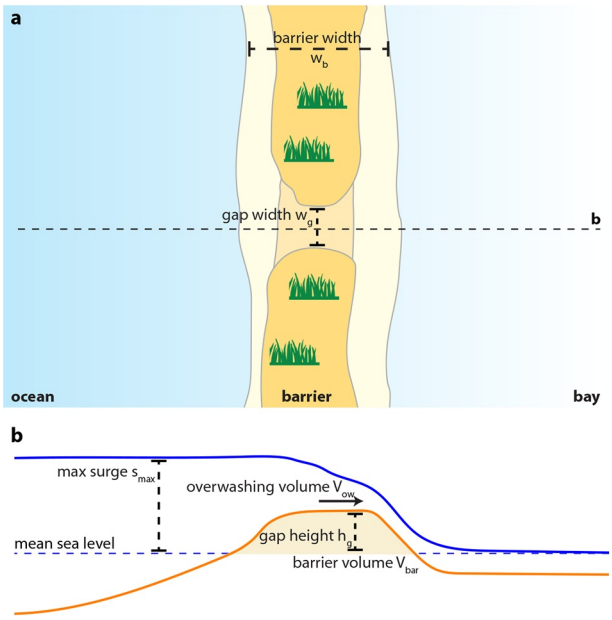

Figure 2. Conceptual model of an overwashing flow through a dune gap. (a) Plan-view barrier island separating the bay from the ocean, (b) cross-section through the dune gap highlighting the overwashing volume Vow and the barrier volume V_{bar}.

Passeri et al., 2018), which can constrict the flow and deepen the throat. Flow acceleration through the throat can also widen the gap (Houser et al., 2008).

Predictions for sediment fluxes during wave overwashing in the absence of currents have been formulated using laboratory studies (Nguyen et al., 2009; Williams, 1978). These formulae show reasonable correspondence to a variety of field settings and highlight a quadratic dependence of wave overwash fluxes to wave runup. A similar wave overwash model from Kobayashi et al. (2010) shows that overwash volumes are sensitive to barrier geometry. Their results are validated by experimental and field evidence but do not include the effect of currents on sediment fluxes. We refer to Donnelly et al. (2006) for a review on overwashing flows, who note explicitly that the morphologic evolution of overwash flows and initiation of breaching remain poorly quantified.

2.2. Washover Deposition

Washovers form through the settling of sediment transported by overwashing flows (Woodruff et al., 2008). A compilation from Hudock et al. (2014) shows large variability in washover area, but many washovers are less than 1 km^2. Carruthers et al. (2013) report washover volumes normalized per unit width alongshore and obtain a median of 30 m^3/m. A scaling analysis of experimental and natural washover deposits finds that they are typically longer (cross-shore) than they are wide (alongshore), with a length/width ratio of ~2 (Lazarus, 2016).

The length and size of washover deposits are controlled by storm characteristics (Morton et al., 2003). Barrier island morphology and land cover such as the type of development or vegetation can affect its response to storms and the character of its washovers (Hayes, 1979; Leatherman, 1979; Rogers et al., 2015; Sedrati et al., 2011). Rogers et al. (2015) find a mean of 62 m^3/m for natural environments but 38 m^3/m and 8 m^3/m for residential and commercially developed islands, respectively. Washovers can compete for flow with their neighbors, which can result in a characteristic spacing of washover deposits (Lazarus & Armstrong, 2015).

2.3. Breaching

Overwashing flows can also lead to barrier island breaching. Many studies of barrier breaching focus on the exposed US East Coast, where storm surges from hurricanes and extratropical storms frequently result in breaches (Kraus & Hayashi, 2005). Ground-penetrating radar images of the North Carolina outer banks show that at least 24% of the modern barrier island chain has been breached (Mallinson et al., 2010). Breaching also occurs along barrier coasts elsewhere, including the Ebro Delta (Sánchez-Arcilla & Jiménez, 1994), California (Kraus et al., 2002), and Florida (Morgan, 2009).

Models generated from breaches of sand dikes (Visser, 2001; Tuan et al., 2008) focus on the expansion of the overwashing throat (or dune gap, Figure 2) and find that breaches originate by head cutting and erosion of the barrier on the lagoon-side of the throat. Basco and Shin (1999) found that surge level differences between ocean and bay, and the resulting water level gradients, regulate flow conditions and are an important predictor of barrier island breaching. The timing and magnitude of surge level differences across an island are controlled by storm characteristics, bay size, distance to neighboring inlets, and other factors. A large time lag between ocean and bay surge peaks makes breaching toward the ocean more likely (Shin, 1996; Smallegan et al., 2016).

Site-specific process-based models of overwashing flows include Delft3D (Deltares, 2014) and XBeach (Elsayed & Oumeraci, 2016; McCall et al., 2010; Roelvink et al., 2009; Van Dongeren et al., 2009), and have been employed to predict breaching. De Vet et al. (2015) applied XBeach to the well-documented "Wilderness" breach on Fire Island, NY and found that bed roughness, including vegetation roughness, is a sensitive and

poorly constrained parameter that is important for properly hindcasting the emergence of a breach. Recent model-coupling between Delft3D and XBeach (e.g., van Ormondt et al., 2020) show promise for forecasting barrier breaching, but accurate, site-specific process-based simulations of overwashing flows and barrier breaches remain challenging.

On a conceptual level, Kraus et al. (2002) postulated that breach susceptibility is controlled by the storm surge water level and is inversely proportional to the tidal range, used as a proxy for barrier island elevation. A modeling study by Nienhuis and Lorenzo-Trueba (2019a) also showed that breaches are more common in micro-tidal settings, in their case because low tidal range makes that existing inlets fill in faster, increasing the potential tidal prism available to new breaches. Their model also suggests that, similar to alongshore competition for washover flow (Lazarus & Armstrong, 2015), there is alongshore competition for tidal flow that results in a characteristic spacing of successful breaches.

Models for long-term (decades-centuries) barrier island dynamics have shown that the persistence of breaches (i.e., lifetime of tidal inlets) is a function of bay size, tidal range, storm climate, and other controls (Kraus, 1998; Nienhuis & Lorenzo-Trueba, 2019b). They do not represent the effect of storms explicitly but rely on overwash and breaching parameterizations. There remains a large gap in model studies between detailed, site-specific simulations of overwashing flows during storms, and large-scale barrier island models.

Here, we try to bridge the gap between process-based site-specific models versus conceptual studies of breaching and washover deposition. We develop an analytical theory of overwashing flows on storm timescales (hours-days) that can aid short-term risk assessment and help parameterize storm impact for long-term morphologic models. We test this theory using an idealized Delft3D model of overwashing flows on storm timescales combined with observations of washovers and breaches from Hurricane Sandy.

3. Analytical Theory

At the heart of our theoretical model, we compare the volume of overwashing sediments (V_{ow}, in m^3) against the subaerial volume of the barrier (V_{bar}, in m^3) (Figure 1). Following Shin (1996), we classify a barrier as breached when erosion reduces the elevation of the barrier to below sea level and there is no subaerial barrier left after the storm.

Next, we aim to predict the volume of overwashing sediments for different storm characteristics, barrier morphologies, and barrier land covers. We make a simplified predictor with two important assumptions. (1) Overwashes flow from the ocean to the bay. Although our analytical theory is symmetrical and can be applied also in reverse, with flows toward the ocean, we do not do that in this study. (2) We neglect sediment input from the shoreface or from alongshore, assuming that overwashing sediments are eroded from the subaerial barrier directly underneath the dune gap. This makes our theory mostly suitable for short-term (storm timescale) analysis and not post-storm recovery. Breaches that we predict will form might fill in or stay open post-storm depending on conditions that are not considered here, such as the tidal prism, or alongshore sediment transport (e.g., Escoffier, 1940).

We predict the overwashing sediment flux and dune gap erosion using a simple sediment transport-based predictor. This predictor is based on steady, uniform flow for bed shear stress (e.g., depth-slope product) and Engelund and Hansen (1967) for the resulting sediment transport. Combining the depth-slope product (ρghS) and Engelund and Hansen (1967) yields the following prediction for overwashing sediment transport through the dune gap $Q_{ow,t}$ ($m^3\ s^{-1}$),

$$Q_{ow,t}(t) = \frac{0.05}{C_f}\left(\frac{\rho ghS}{(\rho_s - \rho)\cdot g \cdot D_{50}}\right)^{2.5} D_{50}\cdot\sqrt{R\cdot g\cdot D_{50}}\cdot w_g, \quad (1)$$

where C_f is a non-dimensional friction factor, ρ is the density of water (~1,000 kg m^{-3}), ρ_s is the density of sand (~2,650 kg m^{-3}), h is the water depth (m), S is the water surface slope (m m^{-1}), g is gravity (m s^{-2}), D_{50} is the median grain size (m), R is the relative density of sand $\left(\frac{\rho_s - \rho}{\rho}, \sim 1.65\right)$, w_g is the dune gap width

(m) and should be considered the alongshore extent of a gap with a dune height gap of h_g (m) as its average elevation.

We include the effects of vegetation on sediment transport by modifying C_f. Following Baptist et al. (2009), the non-dimensional friction factor for emergent vegetation is $C_f = \frac{g}{C_b^2} + \frac{C_d m D h f}{2}$, where C_b ($m^{0.5}\ s^{-1}$) is a Chezy-type bed roughness without vegetation, C_d is a plant drag coefficient, m (m^{-2}) is the vegetation stem density, D (m) is the vegetation leaf width, h is the vegetation height (m), and f is the fraction of the island covered by vegetation.

We estimate the flow depth h midway through the gap as $\frac{1}{2}\left(s_{max} - h_g\right)$, which is the average flow depth between the ocean ($s_{max} - h_g$) and the bay (0), with s_{max} being the maximum surge level (m) (Figure 2b). The water surface slope during the storm can be approximated as the surge level $s(t)$ (m) as a function of time t (s), divided by the barrier width w_b (m).

Combined, we can simplify Equation 1 to,

$$Q_{ow,t}\left(t\right) = \frac{0.05}{C_f}\left(\frac{s_{max} - h_g}{2}\right)^{2.5}\left(\frac{s\left(t\right)}{w_b}\right)^{2.5}\frac{\sqrt{g}}{R^2 D_{50}} \cdot w_g, \tag{2}$$

and write a predictive equation for the integrated eroded sediment volume of the barrier $V_{ow,t}$ (m^3),

$$V_{ow,t} = \int_0^{Tstorm} Q_{ow,t}\left(t\right)dt, \tag{3}$$

where T_{storm} (s) is the duration of the storm.

For a triangular surge time series $s\left(t\right) = s_{max} \cdot \left(1 - \left|\frac{2t}{T_{storm}} - 1\right|\right)$, of which the integral is identical to $s\left(t\right) = s_{max}\frac{t}{T_{storm}}$, $V_{ow,t}$ evaluates to,

$$V_{ow,t} = \frac{0.05}{C_f}\left(\frac{s_{max} - h_g}{2}\right)^{2.5}\left(\frac{s_{max}}{w_b}\right)^{2.5}\frac{\sqrt{g}}{R^2 D_{50}} \cdot w_g \cdot \frac{2}{7}T_{storm}. \tag{4}$$

We expect the barrier to breach if $V_{ow,t}$ exceeds the subaerial barrier volume V_{bar}, where $V_{bar} = \frac{1}{2}h_g \cdot w_b \cdot w_g$. The factor $\frac{1}{2}$ is included because the barrier profile underneath the dune gap is roughly triangular toward the beach and the lagoon (Figure 2b). We write the theoretical normalized overwash volume $V_{norm,t}$ as,

$$V_{norm,t} = \frac{V_{ow,t}}{V_{bar}} = \frac{\frac{0.05}{C_f}\left(\frac{s_{max} - h_g}{2}\right)^{2.5}\left(\frac{s_{max}}{w_b}\right)^{2.5}\frac{\sqrt{g}}{R^2 D_{50}} \cdot w_g \cdot \frac{2}{7}T_{storm}}{\frac{1}{2}h_g \cdot w_b \cdot w_g}, \tag{5}$$

where a barrier is expected to breach if $V_{norm,t} > 1$.

We expect the subaerial barrier to be maintained if $V_{norm,t} \leq 1$. If that is the case and the overwashing sediment flux will deposit as a washover fan, $V_{ow,t}$ will give an indication of the washover fan volume.

3.1. Predictions of Our Analytical Theory

Equation 5 estimates that the overwash volume scales with surge height to the power 5 because it affects the depth of the overwashing flow as well as the water surface slope. Breaching probability scales with barrier width to the power −3.5. It predicts that overwash volumes scale linearly with dune gap width, and that

dune gap width does not affect breaching probabilities. It is relatively straightforward to evaluate and apply in data-poor environments. Although not applied here, it can be adapted to account for varying water levels in the lagoon as well, including tides and surges that lead to flow toward the ocean.

Some of the trends in Equation 5 align with observations from Wesselman et al. (2019), who found that dune height compared to surge elevation is important for sediment fluxes through dune gaps. Other trends do not align. We predict here (Equations 1–5) that dune gap width is linearly related to overwash volumes, and thereby do not account for the effect of flow contraction nor the potential effect of neighboring overwashes that lower water level gradients. Wesselman et al. (2019) found that flow contraction became significant for smaller widths.

Our predictions also do not consider other important processes that occur in overwashing flows such as supercritical flow or wave breaking (Basco & Shin, 1999; Tuan et al., 2008). It neglects the (wave-dominated) erosion and/or formation of a dune gap. Instead, it follows earlier studies that showed that water level gradients are a first-order control on overwashing flows, washover deposition, and barrier breaching (Basco & Shin, 1999; Engelstad et al., 2018; McCall et al., 2010).

4. Methods

We test our theoretical predictions against Delft3D model simulations and observations from hurricane Sandy for varying storm conditions (T_{storm}, s_{max}), barrier morphologies (w_b, h_g), and barrier land cover and vegetation density (both affecting C_f). Delft3D simulations are not meant to reproduce individual Hurricane Sandy overwashing flows. Instead, Delft3D simulations should be viewed complementary to Hurricane Sandy observations. Both serve as a test of our theoretical model. Delft3D provides modeled washover volumes ($V_{ow,d3d}$) and Sandy provides observed washover volumes ($V_{ow,obs}$) that we can compare against the predicted washover volume ($V_{ow,t}$). We will also test if breaches occur for $V_{norm,t} > 1$ by comparing it to $V_{norm,d3d} = \frac{V_{ow,d3d}}{V_{bar}}$ and $V_{norm,obs} = \frac{V_{ow,obs}}{V_{bar}}$.

4.1. Delft3D Model Setup

We simulate the morphodynamics of overwashing flows using the hydrodynamic and morphodynamic model Delft3D (Deltares, 2014). Delft3D couples shallow water equations with sediment transport formulas to simulate morphologic change. We use idealized barrier island geometries and simulate overwashing flows through a dune gap. Storm surge levels and durations are represented as a water level boundary on the ocean side of the domain (Figure 3d).

The model setup is similar to the one used in an earlier study by Nienhuis et al. (2018), who investigated the morphologic evolution of river levee breaches into avulsions and crevasse splays. A notable difference in our study here is that there is no sediment supply from the upstream boundary. Crevasses are fed by river sediments. Our modeled overwashing flows are not fed by sediments from the ocean; our dune gaps therefore cannot heal but instead simply stop expanding when the storm recedes.

The initial bathymetry of the domain consists of a 1 km long coastal barrier and an adjacent lagoon. Barrier widths vary between 150 and 400 m between model runs, with the rest of the 2 km cross-profile modeled as a 3 m deep lagoon (Figure 3). The domain consists of 172 by 112 cells in the cross-shore and alongshore direction, respectively. The resolution ranges from 5 by 5 m near the dune gap to 20 by 20 m along the sides and into the lagoon to speed up the computation (Figure 3c). The dune gap is in the middle of the simulated barrier island. We vary the height and width of the gap between simulations (Table 1) and use a uniform 0.2 mm sand across the barrier and lagoon.

The effect of vegetation is included using the Baptist et al. (2009) "Trachytope" function, which estimates an effective bed roughness depending on the vegetation height and density relative to the water depth (Deltares, 2014). We span a range of values typical for dune grasses (Biel et al., 2017; Cheplick, 2005; Hacker et al., 2019). Vegetation height is 0.5 m, leaf width is 5 mm, stem density is varied between 0 and 200 m^{-2}, and the aerial fraction is between 0% and 20% for different model runs. Note that these simulations are not

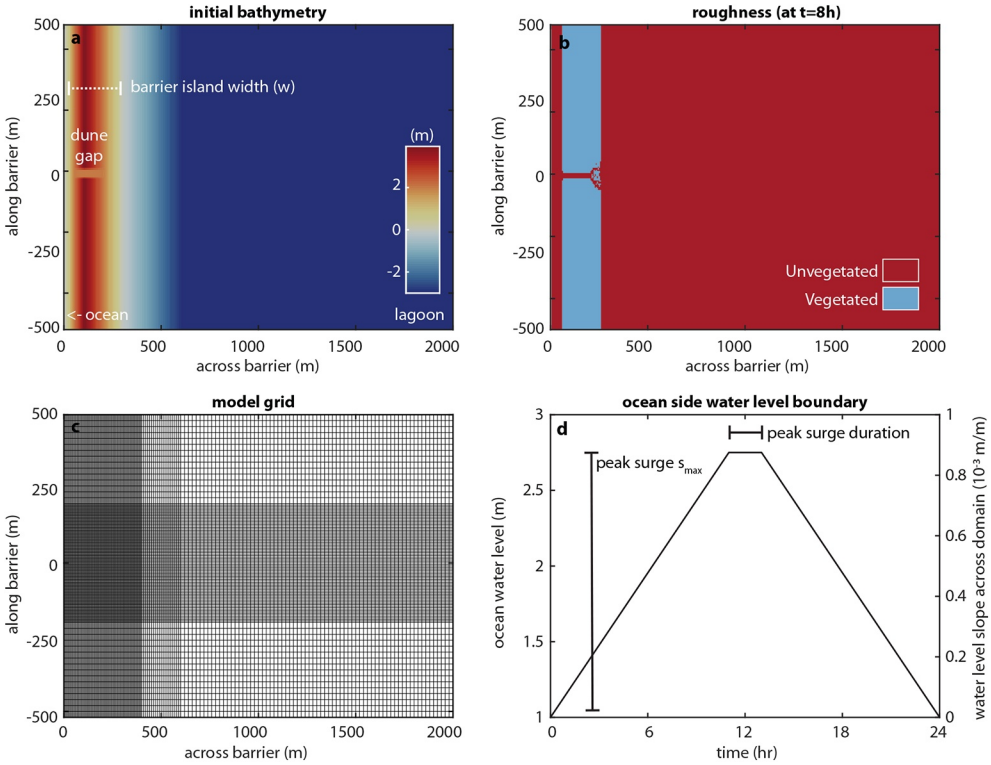

Figure 3. Delft3D model domain and setup to study washover deposition and barrier breaching. (a) Initial bathymetry and barrier morphological parameters, (b) bed roughness (after 8 h of flow to illustrate the model dynamic effects of overwashing flow), (c) model grid cells, and (d) model boundary conditions across the domain. Model setup files and model output are available at https://doi.org/10.17605/OSF.IO/3KNXA.

aimed at representing any specific barrier island, the spread between model scenarios is meant to encompass storm characteristics and barrier island morphologies globally.

The water level boundary condition on the ocean side of the barrier is prescribed as a simplified storm surge lasting 24 h (Figure 3d). We vary the peak surge water level and the duration of the peak between simulation to represent different storm magnitudes. Note that we use a slightly altered surge time series than what is assumed in Equation 4. We therefore use Equation 3 to obtain $V_{ow,t}$ for the Delft3D simulations. The water level at the lagoon is kept constant at 1 m, such that there is no return flow possible through the dune gap. Breaches and washover fans can only appear on the lagoon side of the barrier. There is no flow possible through the side boundaries up and down coast from the breach.

As the water level rises on the ocean side, the dune gap becomes wet and a water surface slope appears across the island. Sediment transport fluxes in Delft3D are calculated following van Rijn (2007), using a 0.1 m water depth threshold for sediment transport for model stability. This is a different sediment transport predictor than what we use in our theoretical model (Equation 1). We choose van Rijn (2007) for our Delft3D simulation because it is more accurate than Engelund and Hansen (1967). We use the latter for our theoretical model because it does not require many parameters and combines bed load and suspended load transport. Dry cells along the edges of the dune gap erode if erosion occurs in the dune gap itself. Delft3D uses a "dry cell erosion factor," set here to the default value of 0.9, that distributes the erosion between wet cells and dry cells. This factor can be viewed as a simple proxy for a critical bed slope for bank failure.

We vary barrier morphology, dune vegetation, and storm characteristics and run 150 model simulations (Figure 3, Table 1). These simulations generate overwashing flows through the dune gap from the water level gradients across the barrier island. Based on this gradient, the barrier width and roughness, and available subaerial barrier volume, morphologic simulations then form either washover deposits or result in barrier breaching. We classify a simulation as "breached" when the maximum elevation of the dune gap thalweg

Table 1
Delft3D Model Simulation Settings

Parameter	Value	Units	Description
S_{max}	2...4	m	Peak surge above MSL
T	0...10	h	Surge duration, different from Tstorm
W	150...400	m	Barrier width
H_g	1...2.5	m	Gap height above MSL
W_g	10...100	m	Gap width
Ocean	f(s,T)	m	Function of storm surge and duration, see Figure 3d
Lagoon	1	m	Lagoon water level boundary
Frac. 1	0...0.2		Fraction of the island using Trachytope 153 (Baptist 1)
Frac. 2	1...0.8		Fraction of the island using Trachytope 105 (Bedforms quadratic)
H_v	0.5	m	Vegetation height
N	0...200	m^{-2}	Stem density
M	5.10^{-3}	m	Leaf width
C_d	1		Drag coefficient of vegetation
C_b	45	$m^{0.5}\ s^{-1}$	Bed roughness chezy
C_f	$4.9.10^{-3}$ ... $2.9.10^{-2}$		Flow roughness (emergent vegetation)
Dryflc	0.1	m	Threshold depth for drying and flooding
EqmBc	0		Equilibrium sand concentration profile at inflow boundaries
SedThr	0.1	m	Minimum water depth for sediment computations
ThetSD	0.9		Factor for erosion of adjacent dry cells
RhoSol	2650	$kg\ m^{-3}$	Specific density
D_{50}	0.0002	m	Median sediment diameter
CdryB	1,600	$kg\ m^{-3}$	Dry bed density

Note. Morphological parameters reflect ranges reported by JALBTCX (coast.noaa.gov/dataviewer/) and Mulhern et al. (2017). Vegetation parameters span the range reported by Cheplick (2005), Biel et al. (2017), and Hacker et al. (2019).

lies below sea level. Reported washover volumes are the sum of post-storm deposition and erosion in the lagoon, not including any subaerial changes on the island tops. We restrict ourselves to washovers in the lagoon for a fair comparison with our Hurricane Sandy analysis, Section 4.2. See Table 1 for an overview of model settings. The supplementary data for the model code and model output to reproduce our findings are available at http://dx.doi.org/10.17605/OSF.IO/3KNXA.

4.2. Hurricane Sandy Analyses

Hurricane Sandy observations allow us to test our theoretical model and our morphodynamic Delft3D simulations. Sandy made landfall on the New Jersey coast on October 29, 2012, and resulted in numerous breaches and washover fans (Sopkin et al., 2014), including the well-documented "Wilderness" breach on Fire Island (van Ormondt et al., 2020). We analyzed 27 overwashing sites, of which 6 resulted in breaches and 21 in overwash fans. Six sites were vegetated, 4 were barren, and 17 were developed. We also retrieved the local storm conditions that led to their formation (Figure 4).

Storm characteristics are determined using the ADCIRC + SWAN hindcast model simulation (Dietrich et al., 2012) via the Coastal Emergency Risk Assessment (CERA), available at www.coastalrisk.live. ADCIRC is a hydrodynamic model that computes time-dependent tide, wind-driven, and pressure-driven surge (Luettich et al., 1992). Coupling with SWAN (Booij et al., 1999) allows for assessment of wave-driven setup. We refer to the documentation of CERA for more information. We use these time-explicit surge hindcasts instead of maximum surge level maps because they allow us to extract water surface slopes.

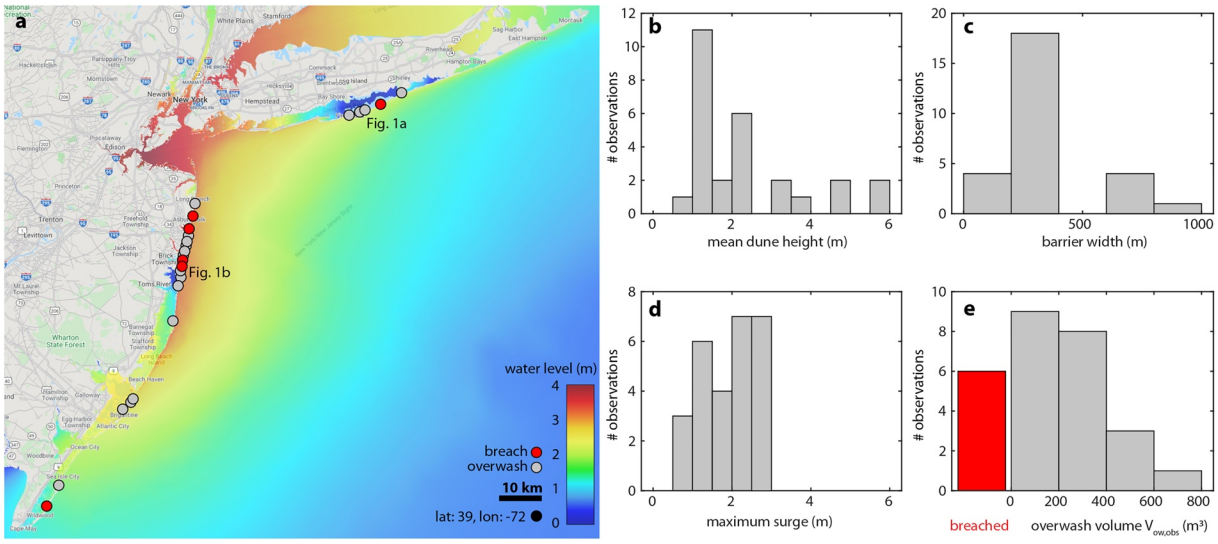

Figure 4. (a) Locations of washovers (gray) and breaches (red) overlain on the maximum water levels during hurricane Sandy. (b)–(e) Distributions of storm and barrier characteristics of the 27 locations.

We extract water levels for the lagoon and ocean sides of the barrier islands at 12, 6, 4, and 0 h before landfall. Unfortunately, CERA does not produce water levels post-landfall, so we assume a symmetric surge event to estimate water levels at 4, 6, and 12 h post landfall. Surge time series are then converted to surge water level differences across the islands, and we interpolate to find the duration where the surge difference exceeded 0.5 m (T_{storm}). The hindcast simulations for Sandy show that the maximum water level differences (s_{max}) between the ocean and lagoon ranged from 0.8 to 2.6 m between sites (Figure 4d).

We use Google Earth images to estimate the pre-storm width and land cover of the overwashing sites. Land cover is categorized as either developed, bare, or vegetated. Roughness coefficients (C_f) for bare and developed land are estimated as $1.6{\cdot}10^{-1}$ and $5{\cdot}10^{-3}$, respectively (Passeri et al., 2018). Vegetated C_f is estimated using Baptist et al. (2009) using bed roughness $C_b = 45\ \mathrm{m}^{0.5}\ \mathrm{s}^{-1}$, stem drag coefficient $C_d = 1$, stem density $m = 20\ \mathrm{m}^{-2}$, leaf width $D = 5$ mm, vegetation height $h = 0.5$ m, and an island fraction covered of $f = 0.2$, resulting in $C_f = 1{\cdot}10^{-2}$.

Dune gap elevations are retrieved from the USGS dune crest elevation data set, which provides mean and standard deviations of dune crest elevation for 1 km alongshore segments (Birchler et al., 2015). Dune gaps are (by definition) lower than these mean elevations. We estimate dune elevations to be Gaussian (following Birchler et al., 2015) and choose the dune gap elevation (h_g) to be the lowest 5% (mean minus 2 SD) of a 1-km alongshore section. Dune gap widths (w_g) are also 5% of the same alongshore segment, here 50 m.

Based on the post-storm NOAA Emergency Response Imagery (https://storms.ngs.noaa.gov/) we characterize each overwashing site as either a breach (e.g., Figure 1a) or a washover deposit (e.g., Figure 1b). We use these same images to measure the subaerial surface area of each washover deposit, contrasting it with pre-storm images. Unfortunately, there is no readily available data to extract washover volumes for the 21 fans in our data set. We use the washover fan data compiled by Lazarus (2016), where field-scale washover volume/area ≈ 0.3 m, to estimate washover volume ($V_{ow,obs}$). For barrier breaches, which do not leave a washover deposit, we set $V_{norm,obs} > 1$. This does not affect our analysis.

5. Results

5.1. Mechanics of Overwashing Flows

We use an example Delft3D simulation of a 300-m wide barrier island to illustrate the model dynamics (Figure 5). In this case, a breach developed in response to a 3 m peak surge that lasted 2 h. Water flowing across the gap resulted in high shear stresses, primarily at the back of the dune gap into the lagoon where the water

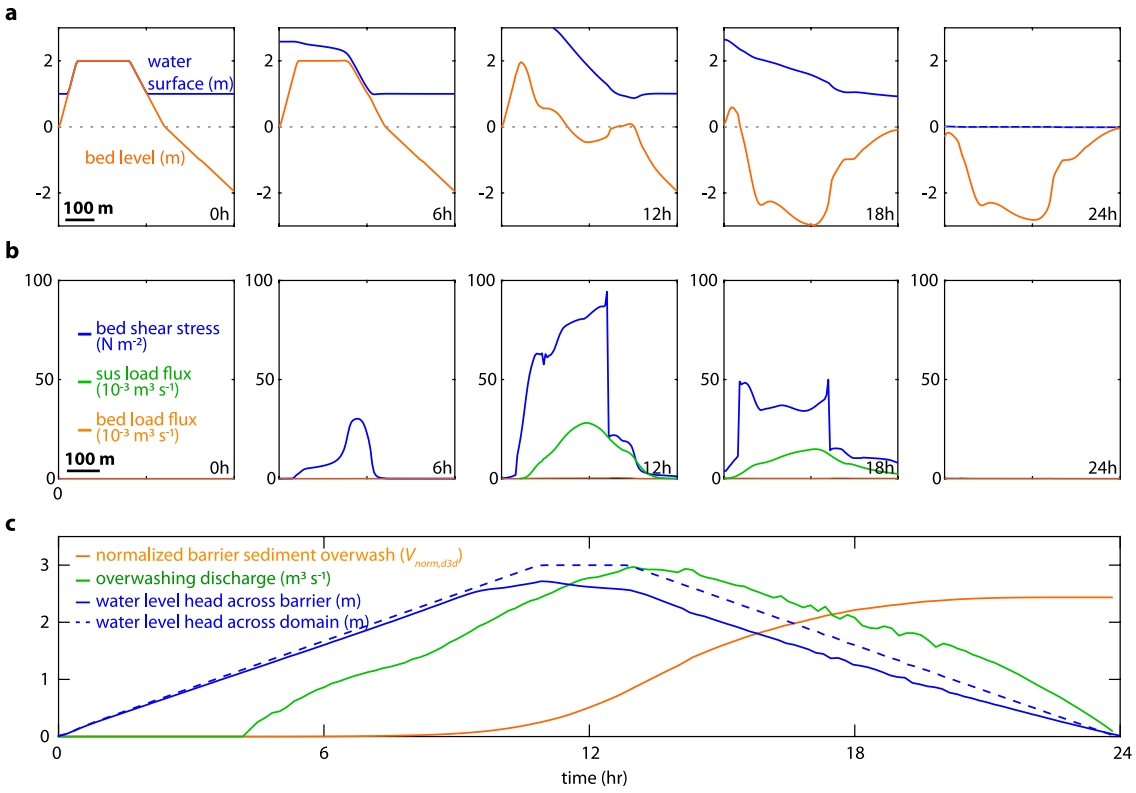

Figure 5. (a) Snapshots of water levels and bed elevation across a dune gap at 0, 6, 12, 18, and 24 h of a 24 h storm surge event that resulted in a breach. (b) Bed shear stress and sediment transport through the dune gap. (c) Time series of water level differences and velocities across the barrier, resulting in a high normalized barrier overwashing flux ($V_{norm,d3d}$) of ~2.4. This indicates that the barrier is likely to be breached.

surface slope is greatest. This agrees with model experiments from Visser (2001). Water level gradients in the lagoon are negligible compared to gradients across the barrier, reflecting the relative flow roughness of both environments (Figure 5c).

Peak shear stresses of ~50 N m^{-2} are observed in the modeled overwashing flows (Figure 5b). Critical shear stress for sand movement, ~0.15 N m^{-2}, is negligible compared to these peak stresses. High concentrations of sediments are suspended and high gradients of sediment transport cause erosion. Suspended transport magnitude greatly exceeds bedload transport, which could be because the Delft3D implementation of Van Rijn (2007) separates bedload and suspended load based on a reference height above the bed. Observations of overwashing flows show that these flows are thin and that sheet-flow conditions are likely, which are usually considered bed load (Shin, 1996).

Simulated overwashing time series show that the greatest transport occurred after the storm surge peak (Figure 5c). Continuous erosion and deepening of the overwash throat led to increasing sediment transport during the event; ~80% of the overwashing sediments were transported in the second half of the storm. The barrier was breached after approximately 20 h.

Comparing the cumulative sediment transported across the barrier island ($V_{ow,d3d}$) with the subaerial volume of the barrier under the overwashing throat (V_{bar}) for our example Delft3D simulation also shows that breaching is likely (Figure 5c). The overwashing flow transported approximately $60 \cdot 10^3$ m^3 of sediment across the barrier. The subaerial barrier is, on average, 1.67-m high, 300-m wide, and the gap extends 50-m alongshore, comprising a volume of $25 \cdot 10^3$ m^3. The result is a normalized barrier overwash $V_{norm,d3d}$ ($V_{ow,d3d}/V_{bar}$) of about ~2.4 at the end of the storm.

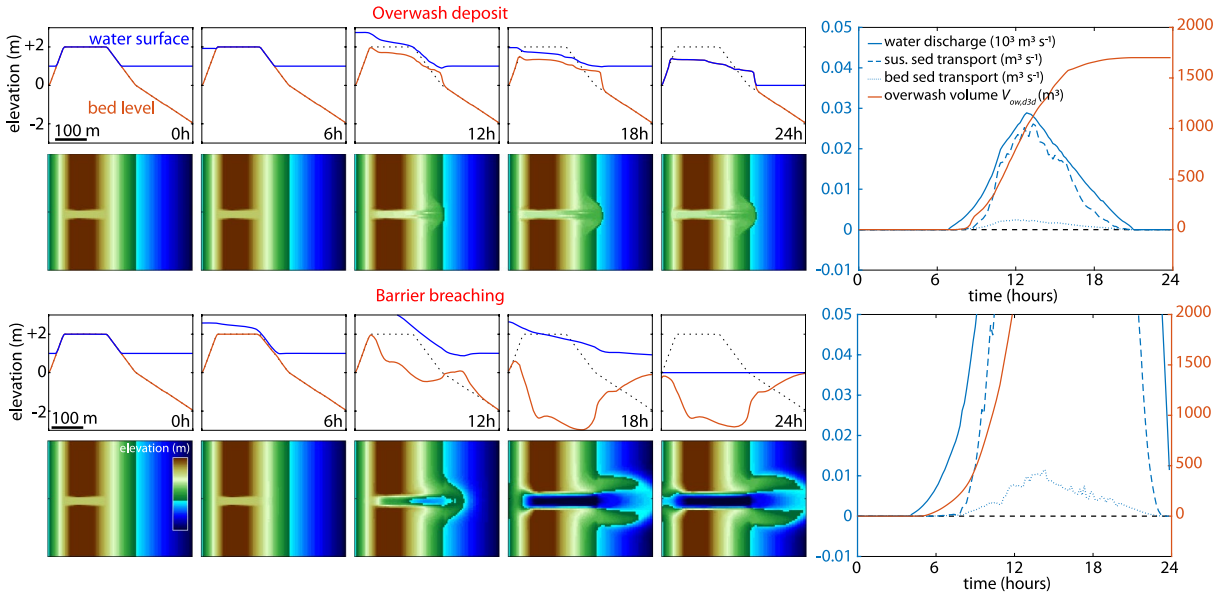

Figure 6. A 2.2 and 3 m peak storm surge resulted in the development of a washover (top panel) and barrier breach (bottom panel, same simulation as Figure 5), respectively. Corresponding figures show the morphologic evolution during the storm and time series of overwashing water and sediment. Dotted lines indicate pre-storm barrier profile.

5.2. Breaching Versus Washover Deposits

We contrast the event from Section 5.1 that resulted in a breach with another simulation where a washover was deposited (Figure 6, bottom panel). The washover formed following a 2.2-m, 2-h long storm surge. Water discharge and suspended sediment transport across the dune gap develop in tandem, and erosion primarily acts on the back of the dune gap. A small, 1,700 m^3 washover fan develops (Figure 6, top panel).

We find similarities between the initial development of the barrier breach and washover deposit: a washover fan also appears in response to the breach, although it is more dispersed spatially (Figure 6, at 12 h, bottom panel). This is intuitive, sediment eroded from a breach must deposit somewhere. Under natural conditions, these deposits could end up being part of a flood-tidal delta, or be transported oceanward during a return flow through the breach (Basco & Shin, 1999).

5.3. Predicting Breach and Washover Events

In 150 simulations we varied storm characteristics and barrier morphologies (Table 1) to better understand controls on washover and barrier breach development. Across all simulations, we find that the overwashing sediment transport fluxes ($V_{ow,d3d}$) range from 0 (no overwash) to $3.3{\cdot}10^5$ m^3. Barrier subaerial volumes (V_{bar}), in comparison, range from $2.6{\cdot}10^3$ to $5.2{\cdot}10^4$ m^3. Normalized overwashing fluxes ($V_{norm,d3d}$) vary between 0 and 12.7.

In 26 simulations the storms resulted in barrier breaches, defined as an open water connection between the ocean and the bay at mean sea level (Figure 7a). For the large majority of the simulations, the threshold $V_{norm,d3d} = 1$ separates storm conditions that lead to barrier washover deposition and barrier breaching. For one simulation we find that a breach occurred despite the normalized overwashing flux $V_{norm,d3d} < 1$ because erosion across the dune gap was not uniform and resulted in a narrow breach. Similarly, for three simulations, internal redistribution of sediments made that the barrier remained intact despite $V_{norm,d3d} > 1$.

Comparing the Delft3D storm impacts ($V_{norm,d3d}$) against predicted storm impact ($V_{norm,t}$, Equation 5) we find that the predictor explains a significant amount of the variation between the model runs ($R^2 = 0.81$, Figure 7b). Washover volumes of Delft3D simulation ($V_{ow,d3d}$) increase for increasing predicted overwashing flux ($V_{ow,t}$). The majority of storms result in barrier breaches when $V_{norm,t} > 1$, and 80% of all simulations

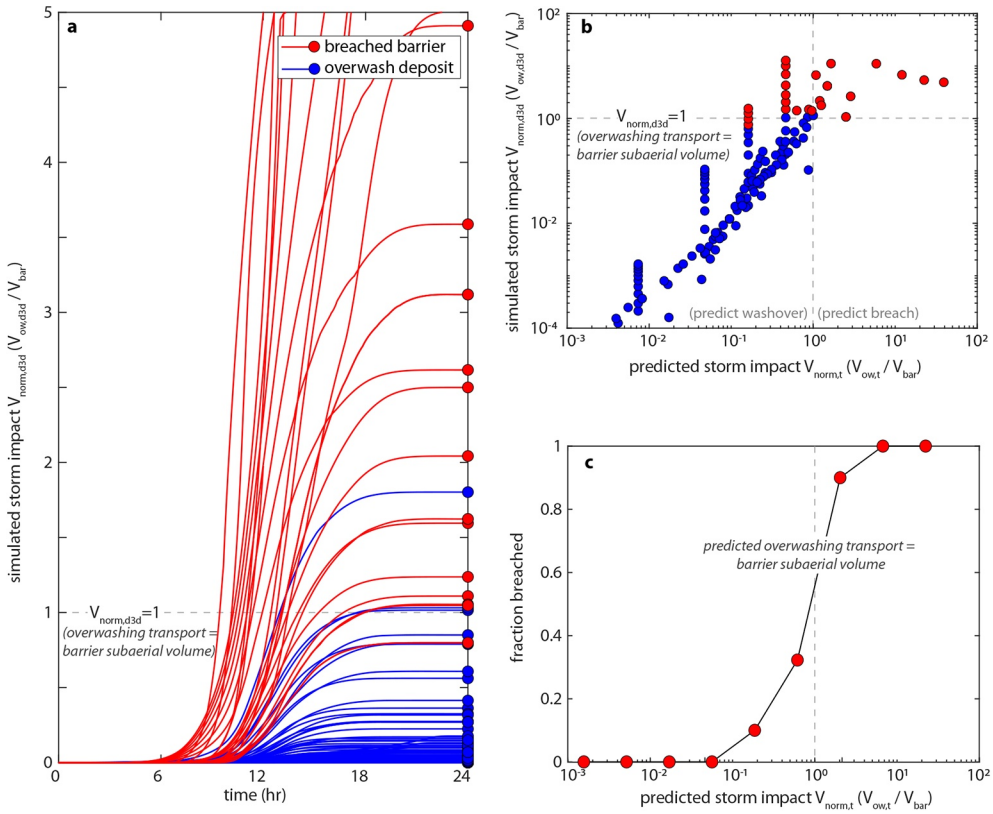

Figure 7. (a) Time evolution of overwashing sediment transport for 150 simulated storms, normalized by the subaerial barrier volume. Red lines indicate simulations where storms led to barrier breaching. Blue lines are simulations resulting in a washover fan. (b) Simulated overwashing sediment flux ($V_{norm,d3d}$) compared to the predicted sediment flux ($V_{norm,t}$). (c) Fraction of simulations resulting in breached barriers as a function of predicted storm impact ($V_{norm,t}$).

result in barrier breaches if $V_{norm,t} > 4$ (Figure 7c). There are inaccuracies as well. 10% of the breaches were in simulations where $V_{norm,t}$ predicted a washover deposit.

Predicted storm impacts $V_{norm,t}$ vary across four orders of magnitude whereas our simulations ($V_{norm,d3d}$) vary across five orders of magnitude, indicating nonlinearities that our (linear) predictor has missed. One nonlinear effect evident in the simulations results from the influence of the dune gap width (w_g) on overwash fluxes. The vertical stacks of experimental results in Figure 7b arise because the dune gap width affects the simulated overwash volumes ($V_{norm,d3d}$) but is canceled out when calculating $V_{norm,t}$ (Equation 5). Our Delft3D simulations show that a linear increase in gap width results in a supralinear increase in overwashing sediment fluxes. The decrease in flow friction for larger gaps outweighs the effect that flow constriction has to increase flow for small gaps. Our simulations are different from findings by Wesselman et al. (2019), who found that flow constriction leads to a relatively large flux for small gaps.

5.4. Comparison Against Observations From Hurricane Sandy

How do the observations from Hurricane Sandy fit within the variability of the Delft3D simulations? First, we find overwash volumes from Hurricane Sandy occupy a narrow range compared to our simulated volumes from Delft3D (Figure 8). This range in observed volumes is also much narrower than what we predict using our analytical model (Equations 4 and 5), and indicates a (relatively) low sensitivity to storm characteristics and barrier morphology. Earlier studies have also noted this and resorted to using a sediment transport limiter (e.g., McCall et al., 2010).

A closer inspection into the Sandy observations shows a large difference between natural and developed coasts. We find that the overwash volumes for developed coastlines are smaller than those along

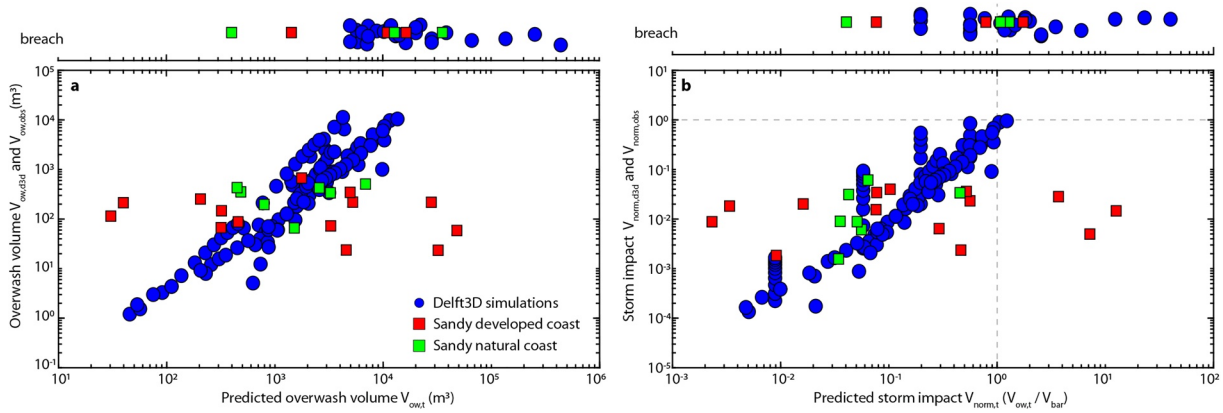

Figure 8. (a) Predicted versus observed overwashing volume and (b) storm impacts for Delft3D simulations and Hurricane Sandy observations. Breaches (which in the case of Sandy observations have no observed overwash volume) are plotted separately, above. The observed variability in storm impacts on developed coasts (red squares) is not captured by our predictor.

undeveloped coasts (mean of 200 and 370 m^3, respectively), although there is a risk of selection or observation bias introduced by post-storm cleanup (e.g., Lazarus & Goldstein, 2019). Other studies have also found a large effect of development on overwash dynamics. Rogers et al. (2015) found a 40% decrease in overwash volumes comparing residential to natural environments. Structures block flow and pavement limits erosion (Lazarus et al., 2021; Rogers et al., 2015).

The magnitudes and trends of Hurricane Sandy overwashes and breaches that formed on natural (undeveloped) coasts are similar to our Delft3D observations (Figure 8). This general agreement highlights the importance of the parameters in our predictor (barrier width, barrier height, and storm surge height) on barrier morphologic response. Two (out of three) breaches were predicted correctly ($V_{norm,t} > 1$ and $V_{norm,obs} > 1$). All of the seven observed washovers were correctly predicted ($V_{norm,obs} < 1$ and $V_{norm,t} < 1$), but there is no statistically significant correlation between the predicted and observed overwash volumes ($V_{ow,obs}$ vs. $V_{ow,t}$).

In contrast to our observations for natural coasts, we do not observe any trends in the breaches and overwash fans that formed along developed coasts (Figure 8). Some of the developed coast breaches had a very low breaching probability ($V_{norm,t} \approx 0.4$), whereas observed overwash fans along developed coastlines formed despite a predicted breach ($V_{norm,t} = 43$).

6. Discussion

In this study, we developed and tested an analytical theory for the development of washover fans and barrier breaches. In general, the simulations and predictors are simplified compared to the natural dynamics of overwashing flows, which allowed us to present an analytic formulation that is integrated over the duration of the storm.

6.1. Analytical Predictor Strengths and Weaknesses

Tests of our theory against Delft3D simulations and Hurricane Sandy observations showed mixed results. Delft3D simulations corresponded well, but natural and developed barrier response to Hurricane Sandy differed from theoretical expectations. Along natural barrier coasts, one observed breach was predicted to be a washover (#10 of Table S1). This occurred near Stone Harbor Point, NJ, on a wide sand flat close to an existing inlet. Likely the tidal conditions created overwashing flow dynamics to behave differently than our theoretical model. Detailed, site-specific simulations with more accurate pre-storm morphology (e.g., van Ormondt et al., 2020) are likely to be better suited to study these individual cases. Comparison against more field data, comprising different storms and different barrier islands, would also help to expand the range of observations and potentially improve the fit to predictions.

Disagreement between developed barrier response and theoretical expectations could indicate that important variables are missing in our model. Perhaps it is the erodibility of pavement or surface heterogeneity that funnels or disperses overwashing flows (Lazarus et al., 2021; Rogers et al., 2015) that dominate the response to storms for developed coasts. Many coasts are developed, so the poor performance of our (fairly traditional) sediment transport predictor indicates a need for morphodynamic formulations and models better suited for these environments.

6.2. Implications for Paleo Environmental Reconstructions

Washover fan deposits are often used to reconstruct storms and climatic conditions (Mulhern et al., 2019; Shaw et al., 2015; Woodruff et al., 2008). Fan size and internal stratigraphy can record storm tracks, but bracketing paleo-storm intensity remains challenging. Our storm impact predictor (Equation 5) can be used as an inverse model to reconstruct paleo-storms where detailed models might not be appropriate because accurate boundary conditions and initial conditions are difficult to obtain. For example, our predictor could indicate a minimum storm intensity that would result in the formation of a washover fan with a certain observed volume or thickness. The presence of a preserved washover fan might also be used as an indication for a maximum storm intensity because the storm did not breach the barrier.

6.3. Implications for Morphodynamic Barrier Island Models

The landward sediment transport of barrier overwashing flows is important for the long-term survival of barrier islands facing sea-level rise (Nienhuis & Lorenzo-Trueba, 2019a; Storms, 2003). Models have been developed to investigate overwashing fluxes and long-term barrier dynamics (Ashton & Lorenzo-Trueba, 2018; Nienhuis & Lorenzo-Trueba, 2019b), but scale discrepancies still exist between our understanding of individual storms and barrier island transgression.

Current state-of-the-art barrier island models (Lorenzo-Trueba & Ashton, 2014) are reliant on empirical concepts that estimate washover deposition based on a distance function away from the current shoreline (Storms et al., 2002) or a certain critical barrier width (Jiménez & Sánchez-Arcilla, 2004; Leatherman, 1979; Rosati & Stone, 2007). This latter concept suggests that washover deposition into the lagoon only occurs if the barrier width is below a certain (critical) width. The overwash flux is then estimated based on how much the barrier width deviates from the critical width, and sometimes is also limited below a certain maximum flux (Lorenzo-Trueba & Ashton, 2014). The shape and limits of these overwash functions are important parameters that affect barrier model persistence under sea-level rise.

Our predictor could help quantify expected overwash fluxes for different storm climates and for future sea levels. The maximum overwash flux concept (Lorenzo-Trueba & Ashton, 2014) is not supported by our Delft3D simulations. That said, a possible maximum (storm-integrated) flux could be the subaerial barrier volume (V_{bar}) itself, as any additional flux would result in a breach. We do find a strong relationship between barrier width and overwashing volume (Equation 4), which, as suggested by the critical width concept, supports a negative feedback that would help barriers retain a certain width (Figure 9a). However, assuming no additional influx from the shoreface or from adjacent dunes, overwash flux exceeding the barrier volume would breach the barrier (Figure 9b) and potentially result in seaward sediment transport through a return current (e.g., Basco & Shin, 1999). The suggested negative feedback that maintains barriers facing sea-level rise through landward transport (Lorenzo-Trueba & Ashton, 2014) may therefore not always hold.

7. Conclusions

In this study, we proposed that barrier islands breach when the cumulative sediment flux of an overwashing flow exceeds the barrier subaerial volume (Equation 5). Washover volumes increase as overwashing flows approach the washover-to-breaching threshold: the largest washover fans likely appear when storms were very close to creating a breach. Tests against idealized Delft3D simulations show good agreement. We find reasonable agreement with observations of natural coastline response to Hurricane Sandy, and no agreement for overwashing across developed coasts. This could be because of the complex erodibility and surface roughness heterogeneity of the built environment.

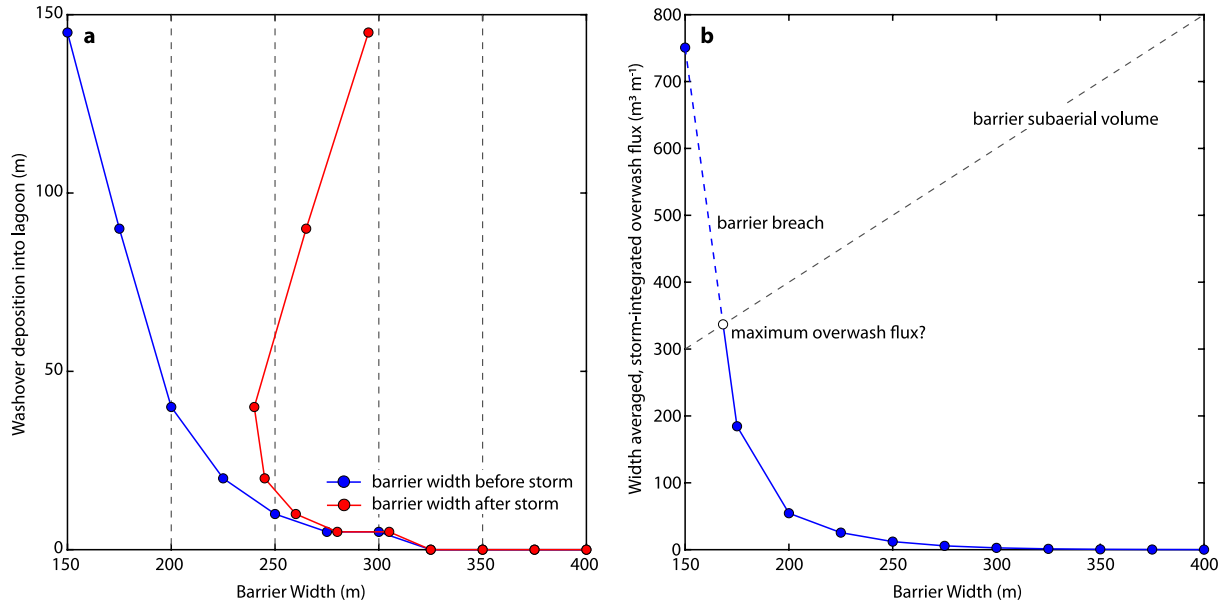

Figure 9. (a) Influence of barrier width on barrier washover distance and post-storm width for a selection of the Delft3D model simulations. Note that the red line is simply the sum of the original width (*x*-axis) and the added washover width (*y*-axis). (b) Influence of barrier width on the alongshore-averaged overwash flux. A alongshore-averaged flux that exceeds the subaerial barrier volume (V_{bar}) results in a breach. This provides some indication that the maximum preserved overwash flux could be equal to the barrier volume.

Our study demonstrates the sensitivity of barrier width and storm surge height on barrier breaching and washover deposition. Increasing storm surge height raises the water depth and water surface slope of overwashing flows. Increasing barrier width reduces the water surface slope and increases the barrier subaerial volume. Barrier height and barrier vegetation reduce the likelihood of barrier breaching, whereas storm duration will increase it. Our predictor could be useful for estimates of barrier landward sediment fluxes in the face of sea-level rise, as well as paleoenvironmental studies of (extra) tropical cyclone dynamics.

Data Availability Statement

Figure S1, model code, and model data to reproduce all findings and figures can be found in the Supporting Information, available at http://dx.doi.org/10.17605/OSF.IO/3KNXA.

Acknowledgments
This study was supported by the Netherlands Organisation for Scientific Research Grant VI.Veni.192.123 to JHN. The authors thank Joe Long for pointing us to useful data on Hurricane Sandy. The authors greatly appreciate the constructive reviewing from an anonymous reviewer, Laura Moore, and Arye Janoff, and editorial work from John Shaw and Amy East.

References

Ashton, A. D., & Lorenzo-Trueba, J. (2018). Morphodynamics of barrier response to sea-level rise. In *Barrier dynamics and response to changing climate* (pp. 277–304). Springer International Publishing. https://doi.org/10.1007/978-3-319-68086-6_9

Baptist, M. J., Babovic, V., Uthurburu, J. R., Keijzer, M., Uittenbogaard, R. E., Mynett, A., & Hoffmann, M. R. (2009). On inducing equations for vegetation resistance. *Journal of Hydraulic Research*, *45*(4), 435–450. https://doi.org/10.1080/00221686.2007.9521778

Basco, D. R., & Shin, C. S. (1999). A one-dimensional numerical model for storm-breaching of barrier islands. *Journal of Coastal Research*, *15*(1), 241–260.

Biel, R. G., Hacker, S. D., Ruggiero, P., Cohn, N., & Seabloom, E. W. (2017). Coastal protection and conservation on sandy beaches and dunes: Context-dependent tradeoffs in ecosystem service supply. *Ecosphere*, *8*(4). https://doi.org/10.1002/ecs2.1791

Birchler, J. J., Dalyander, P. S., Stockdon, H. F., & Doran, K. S. (2015). *National assessment of Nor'easter-induced coastal erosion hazards: Mid- and northeast Atlantic coast*. https://doi.org/10.3133/ofr20151154

Booij, N., Ris, R. C., & Holthuijsen, L. H. (1999). A third-generation wave model for coastal regions 1. Model description and validation. *Journal of Geophysical Research*, *104*(C4), 7649–7666. https://doi.org/10.1029/98JC02622

Carruthers, E. A., Lane, D. P., Evans, R. L., Donnelly, J. P., & Ashton, A. D. (2013). Quantifying overwash flux in barrier systems: An example from Martha's Vineyard, Massachusetts, USA. *Marine Geology*, *343*, 15–28. https://doi.org/10.1016/j.margeo.2013.05.013

Cheplick, G. P. (2005). Patterns in the distribution of American beachgrass (*Ammophila breviligulata*) and the density and reproduction of annual plants on a coastal beach. *Plant Ecology*, *180*(1), 57–67. https://doi.org/10.1007/s11258-005-2467-5

Deltares. (2014). *User manual Delft3D (No. 4.00)*. Deltares. Retrieved from www.delftsoftware.com

De Vet, P. L. M., McCall, R. T., Den Bieman, J. P., Stive, M. J. F., & van Ormondt, M. (2015). Modelling dune erosion, overwash, and breaching at Fire Island (NY) during Hurricane Sandy. In P. Wang, J. D. Rosati, & J. Cheng, Eds., *Paper presented at the Coastal Sediments 2015* (p. 5). World Scientific Pub Co Inc. https://doi.org/10.1142/9789814689977_0006

de Winter, R. C., Gongriep, F., & Ruessink, B. G. (2015). Observations and modeling of alongshore variability in dune erosion at Egmond aan Zee, the Netherlands. *Coastal Engineering*, *99*, 167–175. https://doi.org/10.1016/j.coastaleng.2015.02.005

Dietrich, J. C., Tanaka, S., Westerink, J. J., Dawson, C. N., Luettich, R. A., Zijlema, M., et al. (2012). Performance of the unstructured-mesh, SWAN+ADCIRC model in computing hurricane waves and surge. *Journal of Scientific Computing*, *52*(2), 468–497. https://doi.org/10.1007/s10915-011-9555-6

Donnelly, C., Kraus, N. C., & Larson, M. (2006). State of knowledge on measurement and modeling of coastal overwash. *Journal of Coastal Research*, *22*(4), 965–991. https://doi.org/10.2112/04-0431.1

Elsayed, S., & Oumeraci, H. (2016). Combined modelling of coastal barrier breaching and induced flood propagation using XBeach. *Hydrology*, *3*(4), 32. https://doi.org/10.3390/hydrology3040032

Engelstad, A., Ruessink, B. G., Hoekstra, P., & Vegt, M. (2018). Sand suspension and transport during inundation of a Dutch barrier island. *Journal of Geophysical Research: Earth Surface*, *123*, 3292–3307. https://doi.org/10.1029/2018JF004736

Engelund, F., & Hansen, E. (1967). *A monograph on sediment transport in alluvial streams*. Teknisk Forlag.

Escoffier, F. F. (1940). The stability of tidal inlets. *Shore and Beach*, *8*(4), 114–115.

Fisher, J. S., & Stauble, D. K. (1977). Impact of Hurricane Belle on Assateague Island washover. *Geology*, *5*(12), 765. https://doi.org/10.1130/0091-7613(1977)5<765:IOHBOA>2.0.CO;2

Goff, J. A., Swartz, J. M., Gulick, S. P. S., Dawson, C. N., & de Alegria-Arzaburu, A. R. (2019). An outflow event on the left side of Hurricane Harvey: Erosion of barrier sand and seaward transport through Aransas Pass, Texas. *Geomorphology*, *334*, 44–57. https://doi.org/10.1016/j.geomorph.2019.02.038

Hacker, S. D., Jay, K. R., Cohn, N., Goldstein, E. B., Hovenga, P. A., Itzkin, M., et al. (2019). Species-specific functional morphology of four US Atlantic coast dune grasses: Biogeographic implications for dune shape and coastal protection. *Diversity*, *11*(5), 82. https://doi.org/10.3390/d11050082

Hayes, M. O. (1979). Barrier island morphology as a function of tidal and wave regime. In S. P. Leatherman, Ed., *Barrier islands* (pp. 1–27). Academic Press.

Houser, C., Hapke, C., & Hamilton, S. (2008). Controls on coastal dune morphology, shoreline erosion and barrier island response to extreme storms. *Geomorphology*, *100*(3–4), 223–240. https://doi.org/10.1016/j.geomorph.2007.12.007

Hudock, J. W., Flaig, P. P., & Wood, L. J. (2014). Washover fans: A modern geomorphologic analysis and proposed classification scheme to improve reservoir models. *Journal of Sedimentary Research*, *84*(10), 854–865. https://doi.org/10.2110/jsr.2014.64

Jiménez, J. A., & Sánchez-Arcilla, A. (2004). A long-term (decadal scale) evolution model for microtidal barrier systems. *Coastal Engineering*, *51*(8–9), 749–764. https://doi.org/10.1016/j.coastaleng.2004.07.007

Kobayashi, N. (2010). Wave overtopping of levees and overwash of dunes. *Journal of Coastal Research*, *2010*(265), 888–900. https://doi.org/10.2112/JCOASTRES-D-09-00034.1

Kraus, N. C. (1998). Inlet cross-sectional area calculated by process-based model. In B. L. Edge, Ed., *Paper presented at the Coastal Engineering Proceedings* (pp. 3265–3278). ASCE. https://doi.org/10.9753/icce.v26.%25p

Kraus, N. C., & Hayashi, K. (2005). Numerical morphologic model of barrier island breaching. In *Paper presented at the Coastal Engineering Conference*. https://doi.org/10.1142/9789812701916-0170

Kraus, N. C., Militello, A., & Todoroff, G. (2002). Barrier beaching processes and barrier spit breach, Stone Lagoon, California. *Shore and Beach*, *70*(4), 21–28.

Lazarus, E. D. (2016). Scaling laws for coastal overwash morphology. *Geophysical Research Letters*, *43*(23), 12113–12119. https://doi.org/10.1002/2016GL071213

Lazarus, E. D., & Armstrong, S. (2015). Self-organized pattern formation in coastal barrier washover deposits. *Geology*, *43*(4), 363–366. https://doi.org/10.1130/G36329.1

Lazarus, E. D., & Goldstein, E. B. (2019). Is there a bulldozer in your model? *Journal of Geophysical Research: Earth Surface*, *124*(3), 696–699. https://doi.org/10.1029/2018JF004957

Lazarus, E. D., Goldstein, E. B., Taylor, L. A., & Williams, H. E. (2021). Comparing patterns of hurricane washover into built and unbuilt environments. *Earth's Future*, *9*(3). https://doi.org/10.1029/2020EF001818

Leatherman, S. P. (1979). Migration of Assateague Island, Maryland, by inlet and overwash processes. *Geology*, *7*(2), 104–107. https://doi.org/10.1130/0091-7613(1979)7<104:MOAIMB>2.0.CO;2

Lorenzo-Trueba, J., & Ashton, A. D. (2014). Rollover, drowning, and discontinuous retreat: Distinct modes of barrier response to sea-level rise arising from a simple morphodynamic model. *Journal of Geophysical Research: Earth Surface*, *119*(4), 779–801. https://doi.org/10.1002/2013JF002941

Luettich, R. A., Westerink, J. J., & Scheffner, N. W. (1992). ADCIRC: An Advanced Three-Dimensional Circulation Model for Shelves Coasts and Estuaries, Report 1: Theory and Methodology of ADCIRC-2DDI and ADCIRC-3DL, Dredging Research Program Technical Report DRP-92-6. Dredging Research Program Technical Report DRP-92-6, U.S. Army Engineers Waterways Experiment Station, Vicksburg, MS.

Mallinson, D. J., Smith, C. W., Culver, S. J., Riggs, S. R., & Ames, D. (2010). Geological characteristics and spatial distribution of paleo-inlet channels beneath the outer banks barrier islands, North Carolina, USA. *Estuarine, Coastal and Shelf Science*, *88*(2), 175–189. https://doi.org/10.1016/j.ecss.2010.03.024

McCall, R. T., Van Thiel de Vries, J. S. M., Plant, N. G., Van Dongeren, A. R., Roelvink, J. A., Thompson, D. M., & Reniers, A. J. H. M. (2010). Two-dimensional time dependent hurricane overwash and erosion modeling at Santa Rosa Island. *Coastal Engineering*, *57*(7), 668–683. https://doi.org/10.1016/j.coastaleng.2010.02.006

Morgan, K. L. M. (2009). *Coastal change during Hurricane Ivan 2004*. U.S. Geological Survey Fact Sheet 2009-3026.

Morton, R. A., Sallenger, A. H., Jr, & Sallenger, A. H. (2003). Morphological impacts of extreme storms on sandy beaches and barriers. *Journal of Coastal Research*, *19*(3), 560–573. https://doi.org/10.2307/4299198

Mulhern, J. S., Johnson, C. L., & Martin, J. M. (2017). Is barrier island morphology a function of tidal and wave regime? *Marine Geology*, *387*, 74–84. https://doi.org/10.1016/j.margeo.2017.02.016

Mulhern, J. S., Johnson, C. L., & Martin, J. M. (2019). Modern to ancient barrier island dimensional comparisons: Implications for analog selection and paleomorphodynamics. *Frontiers of Earth Science*, *7*. https://doi.org/10.3389/feart.2019.00109

Nguyen, X.-T., Donnelly, C., Tanaka, H., & Larson, M. (2009). A new empirical formula for coastal washover sediment volume. In *Paper presented at the Coastal Engineering 2008* (pp. 1736–1748). World Scientific Publishing Company. https://doi.org/10.1142/9789814277426_0144

Nienhuis, J. H., & Lorenzo-Trueba, J. (2019a). Can barrier islands survive sea-level rise? Quantifying the relative role of tidal inlets and overwash deposition. *Geophysical Research Letters*, *46*(24), 14613–14621. https://doi.org/10.1029/2019GL085524

Nienhuis, J. H., & Lorenzo-Trueba, J. (2019b). Simulating barrier island response to sea level rise with the barrier island and inlet environment (BRIE) model v1.0. *Geoscientific Model Development*, *12*(9), 4013–4030. https://doi.org/10.5194/gmd-12-4013-2019

Nienhuis, J. H., Törnqvist, T. E., & Esposito, C. R. (2018). Crevasse splays versus avulsions: A recipe for land building with levee breaches. *Geophysical Research Letters*, *45*(9), 4058–4067. https://doi.org/10.1029/2018GL077933

Passeri, D. L., Dalyander, P. S., Long, J. W., Mickey, R. C., Jenkins, R. L., Thompson, D. M., et al. (2020). The roles of storminess and sea level rise in decadal barrier island evolution. *Geophysical Research Letters*, *47*(18). https://doi.org/10.1029/2020GL089370

Passeri, D. L., Long, J. W., Plant, N. G., Bilskie, M. V., & Hagen, S. C. (2018). The influence of bed friction variability due to land cover on storm-driven barrier island morphodynamics. *Coastal Engineering*, *132*, 82–94. https://doi.org/10.1016/j.coastaleng.2017.11.005

Pierce, J. W. (1970). Tidal inlets and washover fans. *The Journal of Geology*, *78*(2), 230–234. https://doi.org/10.1086/627504

Plomaritis, T. A., Ferreira, Ó., & Costas, S. (2018). Regional assessment of storm related overwash and breaching hazards on coastal barriers. *Coastal Engineering*, *134*, 124–133. https://doi.org/10.1016/j.coastaleng.2017.09.003

Roelvink, D., Reniers, A., van Dongeren, A., van Thiel de Vries, J., McCall, R., & Lescinski, J. (2009). Modelling storm impacts on beaches, dunes and barrier islands. *Coastal Engineering*, *56*(11–12), 1133–1152. https://doi.org/10.1016/j.coastaleng.2009.08.006

Rogers, L. J., Moore, L. J., Goldstein, E. B., Hein, C. J., Lorenzo-Trueba, J., & Ashton, A. D. (2015). Anthropogenic controls on overwash deposition: Evidence and consequences. *Journal of Geophysical Research: Earth Surface*, *120*(12), 2609–2624. https://doi.org/10.1002/2015JF003634

Rosati, J. D., & Stone, G. W. (2007). Critical width of barrier islands and implications for engineering design. In N. C. Kraus, & J. D. Rosati, Eds., *Paper presented at the Coastal sediments '07* (pp. 1988–2001). American Society of Civil Engineers. https://doi.org/10.1061/40926(239)156

Sallenger, A. H. (2000). Storm impact scale for barrier islands. *Journal of Coastal Research*, *16*(3), 890–895.

Sánchez-Arcilla, A., & Jiménez, J. A. (1994). Breaching in a wave-dominated barrier spit: The Trabucador bar (north-eastern Spanish coast). *Earth Surface Processes and Landforms*, *19*(6), 483–498. https://doi.org/10.1002/esp.3290190602

Sedrati, M., Ciavola, P., & Armaroli, C. (2011). Morphodynamic evolution of a microtidal barrier, the role of overwash: Bevano, Northern Adriatic Sea. *Journal of Coastal Research*, *64*(ICS2011), 696–700.

Shaw, J., You, Y., Mohrig, D., & Kocurek, G. (2015). Tracking hurricane-generated storm surge with washover fan stratigraphy. *Geology*, *43*(2), 127–130. https://doi.org/10.1130/G36460.1

Shin, C. S. (1996). *A one-dimensional model for storm breaching of barrier islands*. Old Dominion University. https://doi.org/10.25777/3cjy-xw31

Smallegan, S. M., Irish, J. L., Van Dongeren, A. R., & Den Bieman, J. P. (2016). Morphological response of a sandy barrier island with a buried seawall during Hurricane Sandy. *Coastal Engineering*, *110*, 102–110. https://doi.org/10.1016/j.coastaleng.2016.01.005

Sopkin, K. L., Stockdon, H. F., Doran, B. K. S., Plant, N. G., Morgan, K. L. M., Guy, K. K., & Smith, K. E. L. (2014). *Hurricane Sandy: Observations and analysis of coastal change*. (Open-File Report 2014-1088). U.S. Geological Survey.

Storms, J. E. A. (2003). Event-based stratigraphic simulation of wave-dominated shallow-marine environments. *Marine Geology*, *199*(1–2), 83–100. https://doi.org/10.1016/S0025-3227(03)00144-0

Storms, J. E. A., Weltje, G. J., van Dijke, J. J., Geel, C. R., & Kroonenberg, S. B. (2002). Process-response modeling of wave-dominated coastal systems: Simulating evolution and stratigraphy on geological timescales. *Journal of Sedimentary Research*, *72*(2), 226–239. https://doi.org/10.1306/052501720226

Suter, J. R., Nummedal, D., Maynard, A. K., & Kemp, P. (1982). A process-response model for hurricane washovers. In *Paper presented at the Coastal Engineering 1982* (pp. 1459–1478). American Society of Civil Engineers. https://doi.org/10.1061/9780872623736.089

Tuan, T. Q., Stive, M. J. F., Verhagen, H. J., & Visser, P. J. (2008). Process-based modeling of the overflow-induced growth of erosional channels. *Coastal Engineering*, *55*(6), 468–483. https://doi.org/10.1016/j.coastaleng.2008.01.002

Van Dongeren, A., Bolle, A., Vousdoukas, M. I., Plomaritis, T., Eftimova, P., Williams, J., et al. (2009). Micore: Dune erosion and overwash model validation with data from nine European field sites. In M. Mizuguchi, & S. Sato, Eds., *Paper presented at the Coastal Dynamics 2009* (pp. 1–15). World Scientific. https://doi.org/10.1142/9789814282475_0084

van Ormondt, M., Nelson, T. R., Hapke, C. J., & Roelvink, D. (2020). Morphodynamic modelling of the wilderness breach, Fire Island, New York. Part I: Model set-up and validation. *Coastal Engineering*, *157*, 103621. https://doi.org/10.1016/j.coastaleng.2019.103621

van Rijn, L. C. (2007). Unified view of sediment transport by currents and waves. I: Initiation of motion, bed roughness, and bed-load transport. *Journal of Hydraulic Engineering*, *133*(6), 649–667. https://doi.org/10.1061/(ASCE)0733-9429(2007)133:6(649)

Visser, P. J. (2001). A model for breach erosion in sand-dikes In *Paper presented at the Coastal Engineering* (Vol. 276, pp. 3829–3842). American Society of Civil Engineers. https://doi.org/10.1061/40549(276)299

Wesselman, D., de Winter, R., Engelstad, A., McCall, R., van Dongeren, A., Hoekstra, P., et al. (2018). The effect of tides and storms on the sediment transport across a Dutch barrier island. *Earth Surface Processes and Landforms*, *43*(3), 579–592. https://doi.org/10.1002/esp.4235

Wesselman, D., de Winter, R., Oost, A., Hoekstra, P., & van der Vegt, M. (2019). The effect of washover geometry on sediment transport during inundation events. *Geomorphology*, *327*, 28–47. https://doi.org/10.1016/j.geomorph.2018.10.014

Williams, P. J. (1978). *Laboratory development of a predictive relationship for washover volume on barrier island coastlines* (Vol. 54, p. 154). Department of Civil Engineering, University of Delaware. https://doi.org/10.2307/2615542

Woodruff, J. D., Donnelly, J. P., Mohrig, D., & Geyer, W. R. (2008). Reconstructing relative flooding intensities responsible for hurricane-induced deposits from Laguna Playa Grande, Vieques, Puerto Rico. *Geology*, *36*(5), 391. https://doi.org/10.1130/G24731A.1